

Electro-analysis of energetic materials

R. Sivabalan^{a,*}, M.B. Talawar^a, P. Santhosh^b, N. Senthilkumar^b,
B. Kavitha^b, G.M. Gore^a, S. Venugopalan^a

^a High Energy Materials Research Laboratory, Pune 411 021, India

^b Department of Industrial Chemistry, Alagappa University, Karaikudi 630 003, India

Received 18 January 2007; accepted 5 March 2007

Available online 12 March 2007

Abstract

Cyclic voltammetric studies of triaminoguanidine nitrate (TAGN), 3,3'-hydrazino bis(bis[6,6'-(3,5-dimethylpyrazol-1yl)]-1,2,4,5-tetrazine (HBPT), 4,6-dinitrobenzofuroxan (DNBF) and 3,3'-diamino-4,4'-azoxyfurazan (DAAF) were carried out at different pH conditions in 50% aqueous acetonitrile using glassy carbon electrode. Optimum pH was selected for individual compounds. Influence of scan rate and concentration on the voltammetric response were studied in optimum pH. The number of electron transferred was determined by controlled potential coulometry. All compounds undergo diffusion controlled electrochemical reaction. Based on cyclic voltammetric results, differential pulse and square wave voltammetric methods have been developed for the analytical determination. Instrumental parameters such as initial scan potential, amplitude, pulse increment, pulse period, pulse width and frequency were studied. Optimum experimental conditions for each compound were obtained. After fixing optimum conditions, the effect of concentration was studied and calibration plot was arrived. These plots can be used to determine the traces of the above said four energetic materials.

© 2007 Elsevier B.V. All rights reserved.

Keywords: Energetic materials; Trace level determination; Voltammetry; TAGN; HBPT; DNBF; DAAF

1. Introduction

The search for the high-energy materials (HEMs) during the last decade has led to the discovery of a vast number of oxidizers, fuels and explosives with novel and fascinating structure for possible use in rocket propellants and ordnance. With the ever-increasing use of HEMs for both civil and military applications, scientists/technologists are involved in the synthesis and development of new HEMs with modern technologies. In the other hand there is a continuing need for improved analytical methods to yield better sensitivity in the trace level detection of these materials. In recent years identification and quantification of traces of HEMs has constituted an emerging and important topic of interest due to their relevant role in many areas concerning the security and health of the population, including environmental and toxicological effects, land mine detection, aviation security and the prevention of terrorist attacks [1].

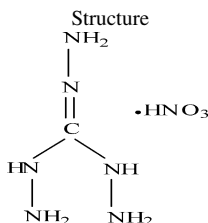
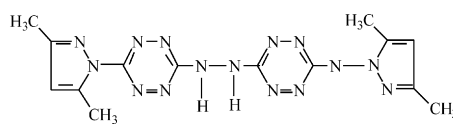
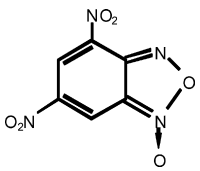
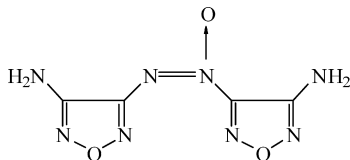
Analytical techniques such as thin layer chromatography [2], high performance liquid chromatography [3], ion mobility spectrometry [4], fast neutron activation analysis [5], capillary chromatography [6], and mass spectroscopy [7] have been used for analysis and detection of explosive compounds.

Electrochemical methods like polarography [8], coulometry [9], amperometry [10], amperometric sensor [11] have been developed for the determination of explosives in soil and water. Cyclic voltammetry analysis for TNT [12], RDX, HMX and PETN were reported [13]. Development of a hand held sensor system with high sensitive technique is desirable for a fast and easy risk estimation of explosive contaminated areas. In view of the increasing importance of HEMs, this study has been undertaken and reports the electrochemical behaviour and electro-analytical procedure developed for the determination of triaminoguanidine nitrate (TAGN), 4,6-dinitrobenzofuroxan (DNBF), 3,3'-diamino-4,4'-azoxyfurazan (DAAF) and 3,3'-hydrazino bis(bis[6,6'-(3,5-dimethylpyrazol-1yl)]-1,2,4,5-tetrazine (HBPT).

Insensitive high explosive (IHEs) is a class of explosives, which significantly improve the safety and survivability of munitions, weapons, and personnel. DAAF is one of the interesting

* Corresponding author. Tel.: +91 20 25869303; fax: +91 20 25869316.
E-mail address: rsivabalan2001@yahoo.co.in (R. Sivabalan).

HEM due to its low vulnerability and high density emanating from planarity of the ring, positive heat of formation, and high percentage of nitrogen content [14]. Similarly, DNBF is also an important HEM, which finds applications in various formulations [15] and its salts used as primary explosives. Triaminoguanidine nitrate is used primarily as an oxidizer in cool burning gun propellants for rapid fire weapon systems [16]. HBPT is an important precursor for making various high nitrogen content high energy materials [17]. All these materials were synthesized on the lines of the reported methods.

Compound name	Structure
Triaminoguanidine nitrate (TAGN)	
3,3'-hydrazino bis(bis[6,6-(3,5-dimethylpyrazol-5-yl)]-1,2,4,5-tetrazine (HBPT)	
4,6-Dinitrobenzofuroxan	
3,3'-Diamino-4,4'-azoxyfurozan (DAAF)	

2. Experimental

2.1. Chemicals

The compounds (TAGN, HBPT, DNBF and DAAF) were synthesized and used for the present study. TAGN is water soluble while others are soluble in acetonitrile. Stock solutions of these materials (0.01 M) were prepared in acetonitrile except TAGN, was prepared in water. Different pH solutions were prepared using H₂SO₄, KCl and KOH. 0.0001 M KOH in 50% aqueous acetonitrile (pH 10) was used as supporting electrolyte. All chemicals used were of analytical reagent grade.

2.2. Instrument and electrode set up

Electrochemical experiments were performed using CH Instrument – 620A Electrochemical Analyzer. A three electrode

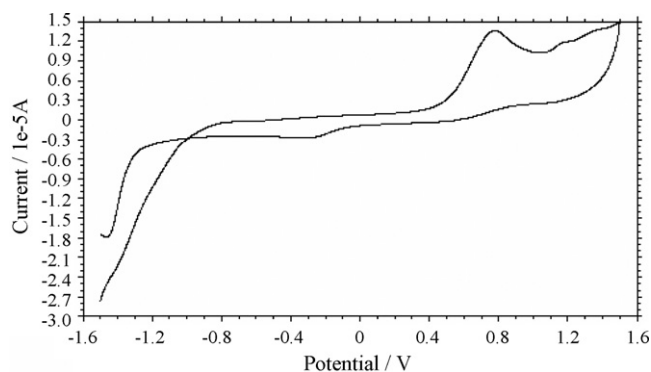


Fig. 1. Cyclic voltammograms obtained for 0.01 M solution of TAGN in deoxygenated aqueous acetonitrile-KOH solution at pH 10; working electrode: glassy carbon, reference electrode: Ag/AgCl and counter electrode: platinum. Scan rate: 50 mV s⁻¹.

cell assembly was used. Glassy carbon, Ag/AgCl and platinum foil were used as working, reference and counter electrodes, respectively. A single compartment cell of 15 cm³ capacity was used in all experiments.

2.3. Electrode pretreatment

The GC electrode was polished with a suspension of alumina powder (1 μm), and then rinsed thoroughly with deionized water to remove any alumina residue. Electrochemical pretreatments were done in a 50 mM (NH₄)₂SO₄ solution, pH 3.0, being adjusted with sulfuric acid. The pretreated electrodes were allowed to stay for 10 min in deionized water before measurements; this procedure improved the stabilization of the voltammetric response. Before each series of measurements, pretreated electrodes were calibrated with a standard solution.

2.4. Procedure

A known volume of the supporting electrolyte solution was taken into the cell, and a known volume of the test solution (analyte) was added into it. A stream of pure nitrogen gas was purged for 15 min before the experiment and then blanketed. Cyclic voltammetry was used for the mechanistic study and stripping voltammetry was used for the analytical determination.

Table 1
Effect of pH on the CV behaviour of TAGN

pH	Peak I (anodic)		Peak II (anodic)	
	E _p (V)	i _p (μA)	E _p (V)	i _p (μA)
1	–	–	1.17	1.08
4	0.67	0.35	1.17	1.14
7	0.89	0.95	1.16	2.68
10	0.80	11.00	1.15	1.04
13	–	–	1.15	5.53

Table 2
Effect of scan rate on CV behaviour of TAGN at pH 10

Peaks	ν $\nu^{1/2}$	10	25	50	75	100	200	300	400	500
Peak I (anodic)	E_p (V)	0.86	0.90	0.85	0.85	0.89	0.99	0.98	0.99	1.00
	$E_{p/2}$ (V)	0.75	0.75	0.74	0.75	0.75	0.83	0.80	0.81	0.83
	$E_p - E_{p/2}$ (mV)	110	150	110	100	140	160	180	180	170
	i_p (μA)	12.31	15.07	22.5	24.8	29.25	38.28	47.92	52.06	61.88
	i_p/ν	1.23	0.60	0.45	0.33	0.39	0.19	0.16	0.13	0.12
	$i_p/\nu^{1/2}$	3.89	3.01	3.18	2.96	2.92	2.91	2.76	2.60	2.76
	αn_a	0.44	0.32	0.44	0.48	0.34	0.30	0.27	0.27	0.28
Peak II (anodic)	E_p (V)	1.23	1.32	1.36	1.37	1.39	1.40	1.41	1.41	1.41
	$E_{p/2}$ (V)	1.16	1.24	1.26	1.29	1.30	1.32	1.33	1.32	1.32
	$E_p - E_{p/2}$ (mV)	70	80	100	80	90	80	80	90	90
	i_p (μA)	0.75	1.35	2.10	2.34	2.63	3.38	4.46	5.75	7.58
	i_p/ν	0.07	0.05	0.04	0.03	0.03	0.02	0.01	0.01	0.01
	$i_p/\nu^{1/2}$	0.22	0.27	0.30	0.27	0.26	0.24	0.26	0.29	0.34
	αn_a	0.69	0.90	0.48	0.60	0.53	0.60	0.60	0.53	0.53

Table 3
Effect of pH on the CV behaviour of HBPT

pH	Peak I (anodic)		Peak II (anodic)		Peak III (anodic)		Peak I (cathodic)		Peak II (cathodic)	
	E_p (V)	i_p (μA)	E_p (V)	i_p (μA)	E_p (V)	i_p (μA)	E_p (V)	i_p (μA)	E_p (V)	i_p (μA)
1	–	–	0.65	5.73	0.90	1.57	0.83	7.26	0.43	8.45
4	0.28	0.60	0.67	2.25	1.02	1.10	0.62	1.63	0.01	5.12
7	0.19	1.89	0.54	1.25	–	–	0.40	1.96	–0.19	9.07
10	0.19	2.45	0.46	4.69	–	–	0.38	3.47	–0.19	3.87
13	0.08	2.50	0.39	9.39	–	–	0.33	4.06	–0.22	5.04

3. Results and discussion

3.1. Cyclic voltammetry behavior of energetic materials

3.1.1. Voltammetric response of TAGN

Fig. 1 shows the cyclic voltammogram recorded for TAGN in the electrolyte solution (pH 10) at the glassy carbon electrode at the scan rate of 50 mV s^{-1} . In weakly basic medium (pH 10), TAGN showed two oxidation peaks at potentials of 0.80 V (peak I) and 1.15 V (peak II). No reduction peaks were observed during

reverse scan of potential. This shows the irreversible nature of the electrochemical reaction. Further, cyclic voltammetric measurements were made in different pHs (1, 4, 7 and 13) at a scan rate of 50 mV s^{-1} . The results obtained are tabulated in Table 1. In strong acidic medium (pH 1), TAGN exhibited one oxidation peak at 1.17 V. However, two peaks were observed at 0.67 V (peak I) and 1.17 V (peak II) at pH 4. In neutral medium (pH 7), TAGN showed two oxidation peaks [0.89 V (peak I) and 1.16 V (peak II)]. Whereas only a single oxidation peak (1.15 V) was observed at pH 13. It is interesting to note that, TAGN did not

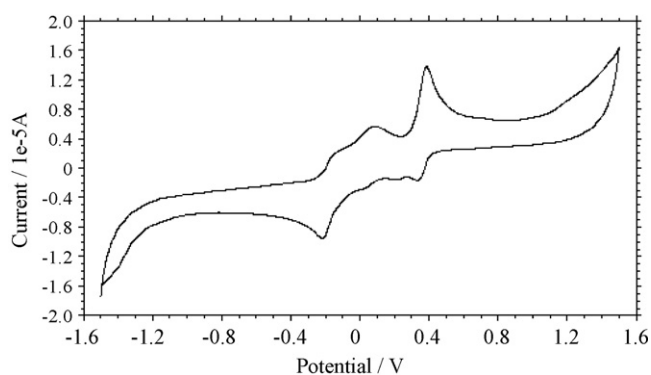


Fig. 2. Cyclic voltammograms obtained for 0.01 M solution of HBPT in deoxygenated aqueous acetonitrile–KOH solution at pH 13; working electrode: glassy carbon, reference electrode: Ag/AgCl and counter electrode: platinum. Scan rate: 50 mV s^{-1} .

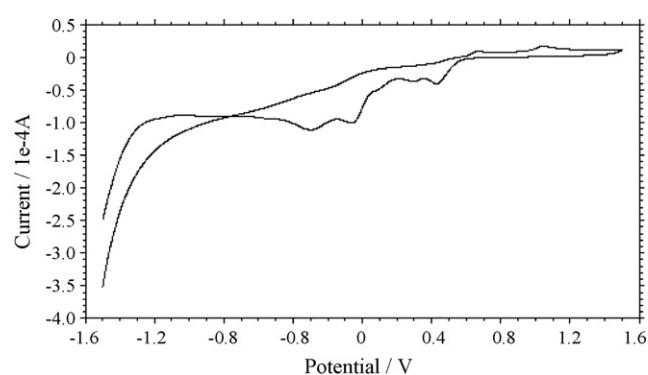


Fig. 3. Cyclic voltammograms obtained for 0.01 M solution of DNBF in deoxygenated aqueous acetonitrile–KOH solution at pH 1; working electrode: glassy carbon, reference electrode: Ag/AgCl and counter electrode: platinum. Scan rate: 50 mV s^{-1} .

Table 4
Effect of scan rate on CV behaviour of HBPT at pH 13

Peaks	ν $\nu^{1/2}$	10	25	50	75	100	200	300	400	500
Peak I (anodic)	E_p (V)	-0.02	-0.01	0.00	0.07	0.07	0.07	0.08	0.08	0.08
	$E_{p/2}$ (V)	-0.17	-0.14	-0.13	-0.08	-0.07	-0.08	-0.02	-0.02	-0.02
	$E_p - E_{p/2}$ (mV)	150	130	130	150	140	150	100	100	100
	i_p (μA)	3.29	3.35	3.85	5.27	6.75	7.12	10.27	11.53	12.47
	i_p/ν	0.33	0.13	0.08	0.07	0.07	0.04	0.03	0.03	0.02
	$i_p/\nu^{1/2}$	1.04	0.67	0.54	0.61	0.67	0.50	0.59	0.58	0.56
	αn_a	0.32	0.36	0.36	0.32	0.40	0.32	0.48	0.48	0.48
Peak II (anodic)	E_p (V)	0.37	0.38	0.39	0.40	0.40	0.40	0.43	0.42	0.42
	$E_{p/2}$ (V)	0.33	0.34	0.34	0.35	0.35	0.36	0.35	0.35	0.35
	$E_p - E_{p/2}$ (mV)	40	40	50	50	50	40	80	70	70
	i_p (μA)	5.03	6.87	8.20	8.62	8.85	10.46	11.05	12.75	13.89
	i_p/ν	0.50	0.27	0.16	0.11	0.08	0.05	0.04	0.03	0.03
	$i_p/\nu^{1/2}$	1.59	1.25	1.16	1.00	0.88	0.74	0.64	0.64	0.62
	αn_a	1.20	1.20	0.96	0.96	0.96	1.20	0.60	0.68	0.68
Peak I (cathodic)	E_p (V)	0.28	0.34	0.35	0.35	0.35	0.35	0.34	0.33	0.34
	$E_{p/2}$ (V)	0.36	0.38	0.40	0.40	0.40	0.40	0.40	0.41	0.42
	$E_p - E_{p/2}$ (mV)	80	40	50	50	50	50	60	70	80
	i_p (μA)	1.50	2.77	3.58	4.21	5.66	7.14	8.40	8.98	9.87
	i_p/ν	0.15	0.12	0.07	0.06	0.05	0.04	0.03	0.02	0.02
	$i_p/\nu^{1/2}$	0.47	0.55	0.51	0.49	0.51	0.51	0.48	0.45	0.44
	αn_a	0.60	1.20	0.96	0.96	0.96	0.96	0.80	0.68	0.60
Peak II (cathodic)	$-E_p$ (V)	0.19	0.18	0.19	0.21	0.22	0.27	0.26	0.26	0.26
	$-E_{p/2}$ (V)	0.13	0.12	0.13	0.12	0.13	0.15	0.15	0.14	0.15
	$E_p - E_{p/2}$ (mV)	50	60	60	90	90	120	110	120	110
	i_p (μA)	5.61	6.81	7.06	7.90	8.75	9.43	10.46	11.54	12.83
	i_p/ν	0.56	0.27	0.14	0.11	0.09	0.05	0.03	0.03	0.02
	$i_p/\nu^{1/2}$	1.77	1.36	1.00	0.91	0.87	0.67	0.60	0.58	0.57
	αn_a	0.96	0.80	0.80	0.53	0.53	0.40	0.44	0.40	0.44

show any reduction waves during the reverse scan of potential at all the pHs studied. This indicates the irreversible nature of TAGN. A high current response and better peak resolution were observed for TAGN when the pH of the electrolyte was kept at 10 and hence, this pH is chosen as optimum for the electrochemical studies.

The effect of scan rate on the voltammetric response of TAGN was studied. Scan rates were varied from 10 to 500 mV s^{-1} in the pH 10. Various parameters such as $E_p - E_{p/2}$ and (n_a) were calculated and presented in Table 2. It is observed that increase in the scan rate resulted in the shift of peak potential (E_p) and half-peak potential ($E_{p/2}$) towards cathodic direction. Further, i_p/ν values showed decreasing trend with scan rate indicating the diffusion control over the reaction and $i_p/\nu^{1/2}$ values

showed almost constancy for both the peaks (peak I and II). There is a linear correlation between the anodic current and the square root of ν in the range of 10–500 mV s^{-1} suggesting that the kinetics of the overall reaction are controlled by diffusion process [18]. Plot of $\log i_p$ versus $\log \nu$ was also made. Slope values of 0.09 and 0.12 were obtained for the two peaks, respectively. The αn values of about 0.5 were obtained for both the peaks. Further the effect of TAGN concentration was studied in the range from 499 to 672 ppm. A linear increase current value with increase in concentration was noted with a correlation coefficient of $r = 0.9982$ with R.S.D. of 0.82%. The current function values were calculated and showed almost constancy. This further indicates the diffusion-controlled nature of the reaction.

Table 5
Effect of pH on the CV behaviour of DNBF

pH	Peak I (anodic)		Peak II (anodic)		Peak I (anodic)		Peak II (cathodic)		Peak III (cathodic)		Peak IV (cathodic)	
	E_p (V)	i_p (μA)	E_p (V)	i_p (μA)	E_p (V)	i_p (μA)	E_p (V)	i_p (μA)	E_p (V)	i_p (μA)	$-E_p$ (V)	i_p (μA)
1	0.66	0.63	1.04	8.47	0.43	37.20	0.29	5.54	0.06	16.46	0.27	12.40
4	0.57	4.52	1.04	1.73	–	–	–	–	0.05	12.24	–	–
7	–	–	1.44	8.57	0.35	17.77	–	–	–	–	0.31	25.02
10	–	–	–	–	–	–	–	–	–	1.95	–	–
13	–	–	–	–	–	–	–	–	0.14	–	0.32	3.26

Table 6
Effect of scan rate on CV behaviour of DNBF at pH 1

Peaks	ν $\nu^{1/2}$	25	50	75	100	200	300	400	500
Peak I (anodic)	E_p (V)	0.66	0.67	0.67	0.66	0.67	0.67	0.68	0.68
	$E_{p/2}$ (V)	0.58	0.62	0.61	0.60	0.62	0.62	0.64	0.64
	$E_p - E_{p/2}$ (mV)	80	60	60	60	50	50	40	40
	i_p (μA)	8.83	9.38	12.71	15.47	15.78	16.93	18.03	20.12
	i_p/ν	0.35	0.19	0.17	0.15	0.09	0.06	0.05	0.04
	$i_p/\nu^{1/2}$	1.77	1.33	1.47	0.55	1.11	0.98	0.90	0.90
	αn_a	0.60	0.80	0.80	0.80	0.96	0.96	1.20	1.20
Peak II (anodic)	E_p (V)	1.03	1.04	1.04	1.03	1.04	1.05	1.08	1.08
	$E_{p/2}$ (V)	0.98	0.99	0.99	0.99	1.00	1.00	1.02	1.02
	$E_p - E_{p/2}$ (mV)	50	50	50	40	40	50	60	60
	i_p (μA)	3.83	7.67	9.34	12.87	16.84	20.25	24.53	27.74
	i_p/ν	0.15	0.15	0.12	0.12	0.08	0.07	0.06	0.05
	$i_p/\nu^{1/2}$	0.77	1.08	1.08	1.24	1.19	1.17	1.22	1.24
	αn_a	0.96	0.96	0.96	1.20	1.20	0.96	0.80	0.80
Peak I (cathodic)	E_p (V)	0.47	0.46	0.47	0.45	0.46	0.46	0.43	0.44
	$E_{p/2}$ (V)	0.53	0.52	0.53	0.52	0.53	0.53	0.50	0.51
	$E_p - E_{p/2}$ (mV)	60	60	60	70	70	70	70	70
	i_p (μA)	34.16	37.41	42.22	49.40	64.52	66.61	69.88	74.32
	i_p/ν	1.37	0.75	0.56	0.49	0.32	0.22	0.17	0.15
	$i_p/\nu^{1/2}$	6.88	5.29	4.87	4.94	4.56	3.84	3.50	3.32
	αn_c	0.80	0.80	0.80	0.68	0.68	0.68	0.68	0.68
Peak II (cathodic)	E_p (V)	0.32	0.31	0.31	0.31	0.30	0.31	0.29	0.29
	$E_{p/2}$ (V)	0.38	0.37	0.37	0.36	0.37	0.37	0.35	0.36
	$E_p - E_{p/2}$ (mV)	60	60	60	50	70	60	60	70
	i_p (μA)	5.00	6.62	8.22	9.24	12.99	14.01	16.12	18.11
	i_p/ν	0.20	0.13	0.11	0.09	0.06	0.05	0.04	0.04
	$i_p/\nu^{1/2}$	1.00	0.94	0.94	0.92	0.92	0.81	0.81	0.81
	αn_c	0.80	0.80	0.80	0.96	0.68	0.80	0.80	0.68
Peak III (cathodic)	$-E_p$ (V)	0.006	0.02	0.02	0.04	0.04	0.05	0.09	0.09
	$E_{p/2}$ (V)	0.06	0.04	0.04	0.02	0.01	0.00	-0.02	-0.02
	$E_p - E_{p/2}$ (mV)	66	60	60	60	50	50	70	70
	i_p (μA)	42.58	57.45	63.78	64.52	66.62	67.71	69.79	70.83
	i_p/ν	1.70	1.14	0.85	0.64	0.33	0.22	0.17	0.14
	$i_p/\nu^{1/2}$	8.52	8.12	7.36	6.45	4.71	3.90	3.50	3.17
	αn_c	0.73	0.80	0.80	0.80	0.96	0.96	0.68	0.68
Peak IV (cathodic)	$-E_p$ (V)	0.22	0.25	0.26	0.26	0.30	0.33	0.40	0.39
	$-E_{p/2}$ (V)	0.16	0.18	0.19	0.19	0.22	0.25	0.33	0.32
	$E_p - E_{p/2}$ (mV)	60	70	70	70	80	80	70	70
	i_p (μA)	12.15	12.60	13.50	18.00	33.33	37.87	39.73	41.09
	i_p/ν	0.49	0.25	0.18	0.18	0.17	0.12	0.09	0.08
	$i_p/\nu^{1/2}$	2.43	1.78	1.55	1.80	2.36	2.19	1.99	1.84
	αn_c	0.80	0.68	0.68	0.68	0.60	0.60	0.68	0.68

3.1.2. Voltammetric response of HBPT

Cyclic voltammetry of HBPT was studied in different pH such as 1, 4, 7, 10 and 13 at a scan rate of 50 mV s^{-1} (Table 3). Fig. 2 shows the cyclic voltammogram recorded for HBPT in

the electrolyte solution (pH 13) at the glassy carbon electrode at the scan rate of 50 mV s^{-1} . HBPT showed two oxidation peaks at potentials of 0.08 V (peak I) and 0.39 V (peak II) and corresponding reduction peaks at 0.33 V (peak I), and 0.22 V

Table 7
Effect of pH on the CV behaviour of DAAF

pH	Peak I (anodic)		Peak II (anodic)		Peak I (cathodic)		Peak II (cathodic)	
	E_p (V)	i_p (μA)	E_p (V)	i_p (μA)	E_p (V)	i_p (μA)	E_p (V)	i_p (μA)
1	–	–	1.14	5.19	0.08	35.02	–	–
4	0.03	5.16	1.20	1.72	–	–	0.44	4.25
7	0.11	5.36	1.29	0.88	0.15	27.58	–	–
10	-0.04	4.02	–	–	0.26	23.15	–	–
13	-0.04	8.45	–	–	0.16	15.35	–	–

Table 8
Effect of scan rate on CV behaviour of DAAF at pH 7

Peaks	ν	10	25	50	75	100	200	300	400	500
	$\nu^{1/2}$	3.16	5.00	7.07	8.66	10.00	14.14	17.32	20.00	22.36
Peak I (anodic)	E_p (V)	0.04	0.06	0.12	0.12	0.16	0.18	0.19	0.21	0.21
	$E_{p/2}$ (V)	-0.07	-0.06	-0.02	-0.01	0.06	0.09	0.09	0.10	0.11
	$E_p - E_{p/2}$ (mV)	110	120	140	140	100	90	100	110	100
	i_p (μA)	6.92	10.20	12.57	14.56	16.06	19.05	22.56	25.65	28.24
	i_p/ν	0.69	0.41	0.25	0.19	0.16	0.10	0.08	0.07	0.06
	$i_p/\nu^{1/2}$	2.19	2.04	1.78	1.68	1.61	1.36	1.30	1.29	1.29
	αn_a	0.44	0.40	0.34	0.34	0.48	0.53	0.48	0.44	0.48
Peak I (cathodic)	$-E_p$ (V)	0.11	0.13	0.13	0.14	0.15	0.15	0.15	0.15	0.15
	$-E_{p/2}$ (V)	0.06	0.06	0.07	0.06	0.07	0.07	0.07	0.08	0.08
	$E_p - E_{p/2}$ (mV)	50	70	60	80	80	80	80	70	70
	i_p (μA)	17.21	24.01	30.03	32.73	37.19	40.16	44.72	50.14	54.46
	i_p/ν	1.92	0.97	0.60	0.44	0.37	0.20	0.15	0.13	0.11
	$i_p/\nu^{1/2}$	5.42	4.80	4.23	3.78	3.70	2.84	2.58	2.51	2.43
	αn_c	0.90	0.68	0.80	0.60	0.60	0.60	0.60	0.68	0.68

Table 9
Optimum experimental conditions obtained in DPSV

Compound	E_{acc} (V)	E_{is} (V)	Amplitude (V)	Increment (V)	Pulse width (s)	Pulse period (s)	t_{acc} (s)
TAGN	1.5	-1.0	0.20	0.008	0.06	0.12	40
HBPT	-1.5	-1.0	0.04	0.004	0.02	0.04	20
DNBF	-1.5	-0.25	0.05	0.006	0.04	0.08	20
DAAF	1.5	-0.75	0.05	0.010	0.04	0.08	20

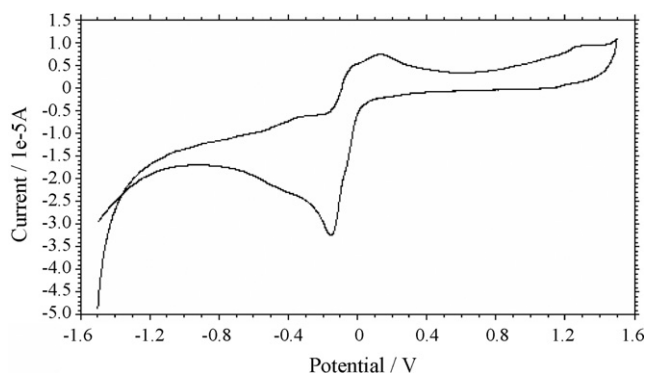


Fig. 4. Cyclic voltammograms obtained for 0.01 M solution of DAAF in deoxygenated aqueous acetonitrile–KOH solution at pH 7; working electrode: glassy carbon, reference electrode: Ag/AgCl and counter electrode: platinum. Scan rate: 50 mV s^{-1} .

(peak II). At pH 1, HBPT exhibited two oxidation peaks, one at 0.65 V (peak II) and other at 0.90 V (peak III) and two reduction peaks at 0.83 V (peak I) and 0.43 V (peak II). However, at pH 4, HBPT showed three oxidation peaks (0.28, 0.67 and 1.02 V) and

corresponding reduction peaks at 0.62 and 0.01 V. At pHs 7 and 10, HBPT showed two oxidation peaks at 0.19 and ~ 0.40 V and two reduction peaks at 0.40 and -0.19 V. Among the pH range studied, pH of 13 showed better peak response resolution and high current value and hence it was taken as optimum.

The effect of scan rate was studied in the range from 10 to 500 mV s^{-1} in the pH 13 and the results are presented in Table 4. As the scan rate was increased, the anodic peak potential (E_p) and half-peak potential ($E_{p/2}$) shifted towards positive direction whereas the cathodic peaks shifted towards negative direction. The peak current i_p values showed increasing trend with scan rate and i_p/ν values showed decreasing trend for all peaks. Further, effect of HBPT concentration was studied in the range from 76 to 108 ppm. As the concentration was increased, the peak current value increased linearly for all the peaks. The current function values calculated showed almost constancy for all peaks. This indicates the diffusion-controlled nature of the reaction.

3.1.3. Voltammetric response of DNBF

Cyclic voltammetry response of DNBF was studied in different pH conditions such as 1, 4, 7, 10 and 13 at a scan rate

Table 10
Optimum experimental conditions obtained in SWSV

Compound	E_{acc} (V)	E_{is} (V)	Amplitude (V)	Increment (V)	Frequency (Hz)	t_{acc} (s)
TAGN	1.5	-0.5	0.10	0.002	20	20
HBPT	-1.5	-1.0	0.05	0.002	20	20
DNBF	-1.5	-0.25	0.04	0.004	8	40
DAAF	1.5	-0.75	0.05	0.008	20	20

of 50 mV s^{-1} . At pH 1, DNBF exhibited two oxidation peaks at 0.66 V (peak I) and 1.04 V (peak II) and four reduction peaks at 0.43 V (peak I), 0.29 V (peak II), -0.06 V (peak III) and -0.27 V (peak IV) (Fig. 3). The peak potential and corresponding peak current values of DNBF at various pHs are presented in Table 5. Among the pH range investigated, pH 1 showed better peak response and high current value for DNBF and hence it was selected for further studies.

The effect of scan rate on the voltammetric response of DNBF was studied. Scan rates were varied from 10 to 500 mV s^{-1} in the pH 1. Various parameters such as $E_p - E_{p/2}$ and (n_a) were calculated and presented in Table 6. The peak current i_p values showed increasing trend and i_p/v values showed decreasing trend for all peaks. The αn value obtained in the scan rate study is in the range between 0.8 and 1.20 for all peaks. The Effect of DNBF concentration was studied in the range from 241 to 326 ppm at a scan rate of 100 mV s^{-1} . As the concentration was increased, the peak current value increased linearly for all peaks. The current function values calculated showed almost constancy for all peaks. This indicates the diffusion-controlled nature of the reaction.

3.1.4. Voltammetric response of DAAF

Cyclic voltammetry of DAAF was studied in different pH conditions (Table 7) and the optimum pH was selected. Among

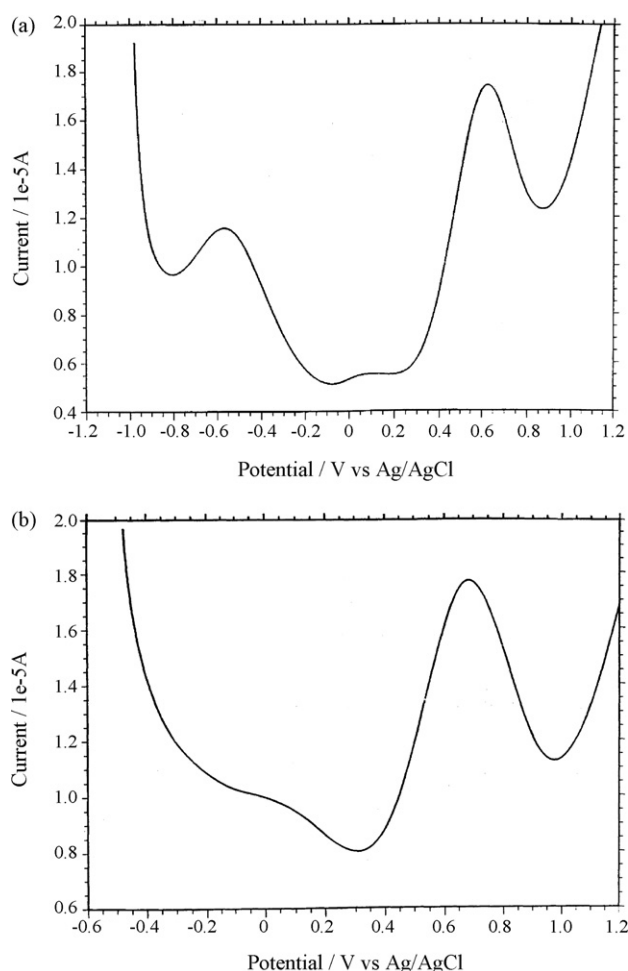


Fig. 5. Stripping voltammograms recorded for TAGN (0.01 M) in the background electrolyte; (a) DPSV and (b) SWSV.

the pH range studied, the pH 7 (Fig. 4) showed better peak response and high current value and hence it was selected for further studies. The effect of scan rate was studied in the range from 10 to 500 mV s^{-1} in pH 7 and various parameters such as $E_p - E_{p/2}$ and n_a were calculated and the results are presented in Table 8. Further, the effect of DAAF concentration was studied in the range from 181 to 248 ppm at a scan rate of 50 mV s^{-1} . As the concentration was increased, the peak current value showed increasing trend. The current function values calculated showed almost constancy for both peaks. This indicates the diffusion-controlled nature of the reaction.

3.2. Stripping voltammetry analysis of energetic materials

Stripping voltammetry is a versatile tool for the determination of analytes at the trace level because of its sensitivity ranging down to sub ppb concentrations [19]. This method is accurate, precise and the instrumentation is of low cost. Stripping voltammetry is a combination of concentration (deposition) step in which the analyte is adsorbed on a solid microelectrode and followed by the step consisting of desorption (stripping) process in which the analyte is removed from the electrode surface. The resulting “stripping voltammogram” shows peaks, the heights of which are generally proportional to the concentration and the potential of which affords qualitative identification of the analyte. In most of the cases, adsorptive stripping voltammetry is employed for the trace analysis of organic compounds exhibiting surface active properties [20,21]. However, a detailed study for the analytical determination of energetic materials by stripping voltammetry is scarce.

3.2.1. Differential pulse stripping voltammetry (DPSV)

The voltammetric analysis at trace levels normally involves a very small current response. For that reason, it is important to optimize all parameters to a high degree of precision. In order to find the best conditions for the adsorption step, several stripping voltammograms were recorded by varying the parameters such as accumulation potentials, E_{acc} (-1.5 to $+1.5 \text{ V}$), pulse amplitudes (0.01 – 0.5 V), pulse increment (0.001 – 0.01 V), pulse width (0.04 – 0.12 s) and pulse period (0.08 – 0.24 s). The effect of accumulation time (t_{acc}) was examined between 20 and 100 s for all compounds. This procedure was extended for all the four compounds. There exists a linear relationship between the peak current and the applied amplitude for all compounds studied. Though higher amplitudes produced the peak with higher current responses, only lower amplitude was selected as optimum because of sharp and narrow peak responses. The optimum conditions obtained for individual compounds are presented in Table 9 and corresponding DPSVs are presented in Fig. 5a, Fig. 6a and b, Fig. 7a and b and Fig. 8a and b.

3.2.2. Square wave stripping voltammetry (SWSV)

Several stripping voltammograms were recorded by varying the accumulation potentials (-1.5 to $+1.5 \text{ V}$), pulse amplitudes (0.01 – 0.4 V), potential increment (0.001 – 0.01 V) and frequency (2 – 30 Hz) for all compounds and an accumulation (t_{acc}) time

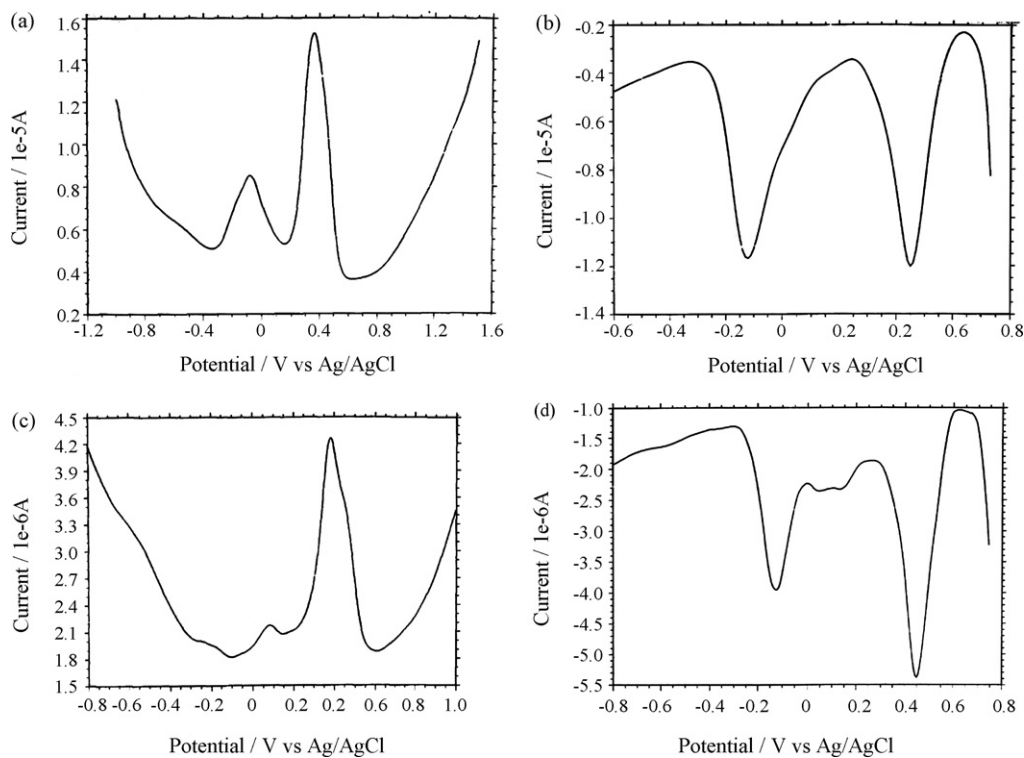


Fig. 6. Stripping voltammograms recorded for HBPT (0.01 M) in the background electrolyte; (a) DPSV, (b) DPSV, (c) SWSV and (d) SWCSV.

between 20 and 100 s was examined for all compounds. The optimum conditions obtained for each compound is presented in Table 10 and corresponding SWSVs are presented in Fig. 5b and Fig. 6c and d, Fig. 7c and d and Fig. 8c and d.

With the optimized conditions, differential pulse (DPSV) and square wave (SWSV) stripping voltammograms were recorded for different concentrations of individual compounds. Linear calibration plots were obtained in the range between 20 and

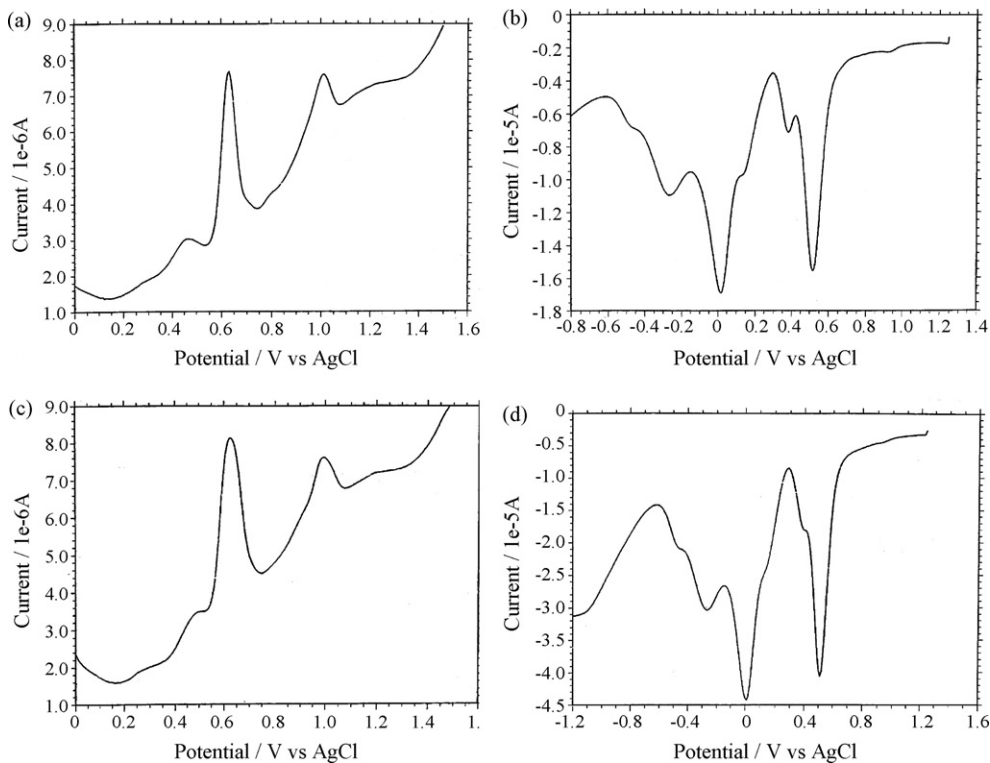


Fig. 7. Stripping voltammograms recorded for DNBF (0.01 M) in the background electrolyte; (a) DPSV, (b) DPSV, (c) SWSV and (d) SWCSV.

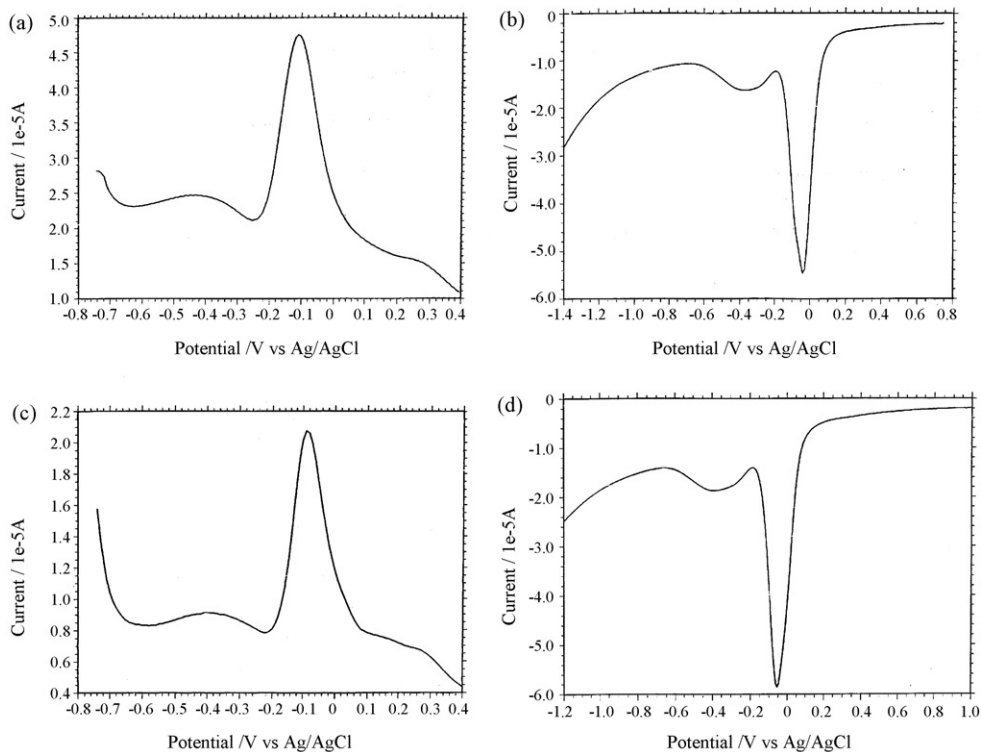


Fig. 8. Stripping voltammograms recorded for DAAF (0.01 M) in the background electrolyte; (a) DPSV, (b) DPSV, (c) SWSV and (d) SWCSV.

90 ppm for all individual compounds. Works are underway for the determination of TAGN, HBPT, DNBF and DAAF contaminants in the soil sample.

3.3. Chronocoulometry

Chronocoulometric experiments were carried out for the compounds with glassy carbon working electrode [22]. The potential of the GC electrode was stepped from an initial potential where no redox reaction occurs to a final potential where the reaction of interest does occur. Instead of measuring current directly, it is integrated and the charge is measured in this

technique. The number of electrons involved in the electrochemical reaction was derived from the forward slope charge value (Q_d) of Anson's plot (Q against $t_{1/2}$) obtained in this experiment using the following equation

$$Q_d = 2nFAD^{1/2}C_t^{1/2}/\pi^{1/2}$$

where n = eq./mole, F = the Faraday constant (96,500), A = area of the electrode (0.0707 cm^2), D = diffusion coefficient in cm^2/s , C = bulk concentration in mol/cm^3 and t = time in seconds. For each compound, the charge (Q_d) was calculated from the Anson's plot and used for the calculation of the number of electrons involved in the reduction process. The number of

Table 11
Results from chronocoulometry measurements

Compound	Peak	Stepping potentia		Forward slope ($\times 10^{-6} \text{ C}$)	Calculated ' D ' value ($\times 10^{-6} \text{ C}$)	Calculated ' n ' value
		Initial (V)	Final (V)			
TAGN	Peak III (anodic)	0.00	0.84	33.81	0.207	2.12
	Peak I (anodic)	-0.30	0.00	1.98	0.1818	2.53
HBPT	Peak II (anodic)	0.30	0.50	7.09	0.6510	2.81
	Peak I (cathodic)	0.50	0.30	3.38	0.3103	2.68
	Peak II (cathodic)	0.00	-0.30	21.51	1.9790	2.26
	Peak I (anodic)	0.50	0.70	4.05	0.5313	1.44
	Peak II (anodic)	0.85	1.25	11.44	1.5007	1.68
	Peak I (cathodic)	0.60	0.30	13.87	1.8195	0.69
DNBF	Peak II (cathodic)	0.40	0.10	14.40	1.8890	1.89
	Peak III (cathodic)	0.20	-0.10	34.24	4.4920	0.63
	Peak IV (cathodic)	-0.10	-0.35	40.75	5.3457	1.46
	Peak I (anodic)	-0.20	0.20	12.04	0.246	3.040
DAAF	Peak I (cathodic)	0.30	-0.30	97.25	1.984	0.978

electrons transferred during oxidation/reduction process and diffusion coefficient values for TAGN, HBPT, DNBF and DAAF were calculated from chronocoulometry experiments are tabulated in Table 11.

4. Conclusions

The compounds triaminoguanidine nitrate (TAGN), 3,3-hydrazino bis[bis[6,6-(3,5-dimethylpyrazol-yl)]-1,2,4,5-tetrazine (HBPT) 4,6-dinitrobenzofuroxan (DNBF) and 3,3'-diamino-4,4'-azoxyfuran (DAAF) studied in the present study are electro active and undergo electrochemical reactions. Methods based on different electro analytical techniques have been developed for the determination of these energetic materials. Determination at ppm level is highly attainable. The stripping voltammetry scan takes hardly few seconds for the analysis of a test sample. The procedure is simple and can be taken to field for real sample analysis. All these results demonstrate the validity of the stripping voltammetric method for the determination of these compounds (TAGN, HBPT, DNBF and DAAF) at low concentration levels, which may be used in environmental monitoring and quality control aspects.

References

- [1] A.M. Jimenez, M.J. Navas, *J. Hazard. Mater.* 106A (2004) 1.
- [2] J. Bladec, R. Andrzej, M. Maciej, *Proc. Int. Pyrotech. Semin.* (1997) 105.
- [3] Huang, Zhi-ping. Cao. Qing-wei. Gao, Xing-ling. *Peop. Rep. China Han-neng Cailiao* 9 (2001) 44.
- [4] S.E. Klassen, P. Rodacy, R.K. Silva, Sandia Natl. Lab. Tech. Rep. (1997) 1.
- [5] S.P. Panda, S.G. Kulkarni, S.K. Sahu, V.N. Bhoraskar, P.A. Dokhale, *J. Energ. Mater.* 16 (1998) 309.
- [6] M.T. Chow, J. Liu, M. Piwoni, R.N. Adrian, *J. Capillary Electrophor.* 4 (1997) 189.
- [7] M.E. Sigman, Ch.Y. Ma, *J. Forensic Sci.* 46 (2001) 6.
- [8] J. Asplund, *J. Propel. Explos. Pyrotech.* 11 (1986) 69.
- [9] P. Janderka, O. Fischer, E. Fischerova, *Collect. Czech. Chem. Commun.* 62 (1997) 581.
- [10] Y. Ai-min, Hong-yuan. C, *Anal. Lett.* 30 (1997) 599.
- [11] M. Krausa, K. Schorb, S. Krebs, F. Beckar, *Ge. DE* 124 (1999) 19748.
- [12] M. Krausa, J. Doll, K. Schorb, W. Boke, G. Hamhitzer, *Propel. Explos. Pyrotechn.* 22 (1997) 156.
- [13] M. Krausa, K. Schorb, *J. Electro. Anal. Chem.* 10 (1999) 461.
- [14] D. Chavez, L. Hill, M. Hiskey, S. Kinkead, *J. Energet. Mater.* 18 (2000) 219.
- [15] B.T. Fedoroff, O.E. Sheffield, *Encyclopedia of Explosives and Related Items*, vol. 2, Picatinny Arsenal, New Jersey, USA, pp. B 68–69.
- [16] S.M. Kaye, *Encyclopedia of Explosives and Related Items*, vol. 9, US Army Armament Research & Development command, New Jersey, USA, pp. T 28–29.
- [17] D.E. Chavez, M.A. Hiskey, R.D. Gilardi, *Angew. Chem. Int.* 39 (2000) 1791.
- [18] L. Zhang, S. Dong, *J. Electroanal. Chem.* 568 (2004) 189.
- [19] D. Melamed, *Anal. Chim. Acta* 532 (2005) 1.
- [20] D.E.M.M. Vendrig, J.J.M. Holthuis, *TrAC Trends Anal. Chem.* 8 (1989) 141.
- [21] A. Arranz, S. Fdez de Betoño, J.M. Moreda, J.F. Arranz, *Talanta* 45 (1997) 417.
- [22] F. Wang, S. Hu, *J. Electroanal. Chem.* 580 (2005) 68.